R2poweR: The Proof-of-Concept of a Backdrivable, High-Ratio Gearbox for Human-Robot Collaboration

Lopez Garcia, Pablo; Crispel, Stein; Varadharajan, Anand; Saerens, Elias; Vanderborght, Bram; Verstraten, Tom; Lefeber, Dirk

Published in:
2022 IEEE International Conference on Robotics and Automation, ICRA 2022

DOI:
10.1109/ICRA46639.2022.9811923

Publication date:
2022

Document Version:
Accepted author manuscript

R2poweR: The Proof-of-Concept of a Backdrivable, High-Ratio Gearbox for Human-Robot Collaboration*

P. L. Garcia, S. Crispel, A. Varadharajan, E. Saerens, T. Verstraten, B. Vanderborght, D. Lefeber

Abstract— **Robotic engineers face major challenges to solve the complex actuation needs of Human-Robot Collaboration with existing act robotic gearboxes. Available technologies comprise high-ratio Planetary Gearheads, Cycloid Drives and Harmonic Drives, inherited from conventional industrial robotics. Alternative approaches include Direct-Drive and Quasi Direct-Drive actuation strategies, which propose to cancel or substantially reduce gear ratio, in order to minimize reflected inertia and attain enough backdrivability for collaborative tasks.**

This paper presents the proof-of-concept validation of a novel high-ratio, Wolfrom-based, gearbox technology that follows a different approach to attain the same objective. Testing five different gearbox prototypes, we confirm the ability of the R2poweR technology to improve efficiency and backdrivability while retaining the weight and control advantages derived from the use of high reduction ratios. The result is a highly efficient, backdrivable, high-ratio gearbox with exciting Huma-Robot Collaboration potential.

I. INTRODUCTION

Industrial robots systematically incorporate high-ratio (typically 60:1 to 120:1) Cycloid Drive (CD) and Harmonic Drive (HD) gearboxes in their joints. Their high positioning accuracy matches with the highly structured environments of industrial robots, while high gear ratios allow for lighter and more compact actuators and minimize the coupling effects between the robot's links, enabling independent control of each joint [1]. The arrival of professional service robots is altering this paradigm: with a +30% growth in 2019, service robots represent today over USD 11 billion [2] and are rapidly broadening beyond traditional robotic application fields. In contrast to conventional industrial robots, service robots typically need to collaborate directly with humans, operating in unstructured environments. Consequently, their actuation needs differ significantly from those of traditional robots [3].

Backdrivability characterizes the ability of an actuator to operate in reverse direction (driven from its output) [4]. In a service robot, backdrivability is directly linked to transparency and thus to basic collaborative functionalities including safety, wearability, or a robot's ability to be manually programmed by demonstration. This makes backdrivability, together with weight and compactness, central aspects of an actuator in collaborative applications [5]. CD and HD gearboxes have high gear ratios and moderate efficiencies that result in high starting torques [6]. To achieve transparency, they depend upon elastic elements or complex active-compliance control techniques, combined with expensive torque sensors.

Direct-Drive actuation strategies renounce using gearing reduction and promise to achieve outstanding dynamic capabilities and backdrivability [7]. Unfortunately, they lead to excessive weight for most service robots and introduce additional control challenges [8], [9]. Several prominent researchers advocate for a compromise solution: Quasi Direct-Drive uses moderate gear reductions (<25:1) to balance lightweight, dynamic, and backdrivability performances. The leg prosthesis of the Texas University at Dallas [10] and MIT's cheetah proprioceptive actuator of [11] are prominent examples of the substantial potential of this actuation strategy.

R2poweR is a patent-pending gearbox technology that explores a different actuation strategy for human-robot collaboration, combining high gear ratios and high efficiency. Previous research [12], [13] demonstrates the potential of efficiency-optimizing tooth macro-geometry for compound Wolfrom (3K) planetary gearboxes [3], Fig.3. The contribution of this paper consists of using five proof-of-concept (PoC) prototypes to empirically demonstrate how novel Wolfrom topologies reduce rolling power and further improve efficiency, removing a main obstacle for the broader use of Wolfrom gearboxes. It enables lighter actuators with improved torque density and backdrivability, taking advantage of the high reduction ratios and compactness of these devices.

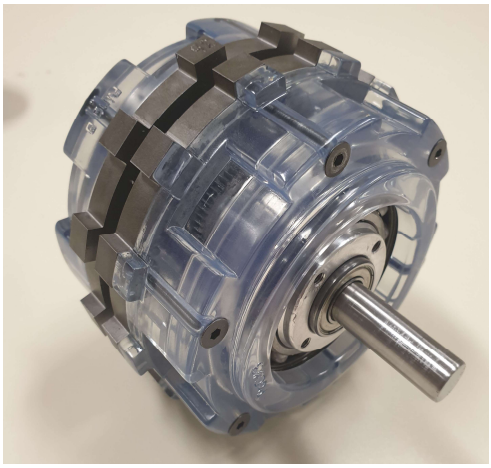

Figure 1.PoC#5, a proof-of-concept gearbox (Φ98 x 68 mm, 1.56kg).

Research supported by the INNOVIRIS Foundation of the city of Brussels, Grant Nr. *2020-POC-03*.

Stein Crispel, Elias Saerens and Tom Verstraten are all funded by the Research Foundation Flanders (FWO). Stein Crispel and Elias Saerens as SB PhD Fellows and Tom Verstraten as a Postdoctoral Fellow.

All authors are with the Robotics & Multibody Mechanics group of the Vrije Universiteit Brussel. Brussels, 1050 Belgium.

Bram Vanderborght is affiliated with IMEC (Leuven, 3001 Belgium), all other authors are affiliated with Flanders Make (Leuven, 3001 Belgium).

Corresponding Author: Pablo Lopez Garcia +32 499741816; plopezga@vub.be

This paper is organized as follows: Section II summarizes the main aspects of the *R2poweR* technology and describes five gearboxes used for its proof-of-concept (TRL4) demonstration. In section III, the methodology and the testbench built for this validation are introduced. Section IV summarizes the results, while sections V and VI respectively discuss our conclusions and future research objectives.

II. Concept

A. A. Operating Principle

R2poweR builds on a largely forgotten technology invented in 1912 by U. Wolfrom [14] and capable of producing very high gear-ratios very compactly. In this gearbox, size depends mainly on output torque and is not significantly affected by gear ratio, contrary to customary planetary gearboxes. This allows a substantial improvement of torque density: for a given payload, increasing gear ratio enables a generous reduction of the input torque and thus of the weight and size of the electrical motor [15], [16], while the gearbox undergo only modest weight and size adjustments.

Unfortunately, Wolfrom gearboxes are also characterized by substantial losses traditionally hindering its adoption in power transmission solutions, restricting its use to applications where efficiency is less relevant [17]. This is a major obstacle for service robots, particularly for those powered by batteries.

Gearbox losses can be classified depending on the element in which they are originated, differentiating into load-dependent and load-independent losses [18]:

$$P_V = P_{VZ} + P_{VZ0} + P_{VB} + P_{VB0} + P_{VD} + P_{VX};$$

Where P denotes power, V = losses, Z = gear mesh, B = bearing, D = sealings, X = others, and subscript 0 identifies load-independent losses in gear meshings and bearings. Of these, load-dependent losses in the gear mesh (P_{VZ}) are mainly responsible for Wolfrom's low efficiency at high-ratios [19], and they can estimated using Ohlendorf's model [20]:

$$P_{VZ} = \mu_{mZ} \cdot F_{bt} \cdot v_{tb} \cdot \frac{\pi \cdot (u \pm 1)}{Z_1 \cdot u \cdot \cos\ _b} \cdot (1\ -\ \varepsilon_\alpha + \varepsilon_1^2 + \varepsilon_2^2);$$

where μ_{mZ} is the friction coefficient, averaged along the contact path, F_{bt} is the tangential force and v_{tb} the tangential relative speed at pitch diameter, u is the number-of-teeth ratio between meshing gears, Z_1 is the number of teeth in the pinion gear, β_b is the base cylinder helix angle, and $\varepsilon_\alpha, \varepsilon_1$ and ε_2 are respectively total, approach, and recess contact ratios.

In a Wolfrom gearbox, both tangential force F_{bt} and relative speed v_{tb} are significant in the Pa-Ra and Pb-Rb meshes (*PoC#1* on Fig.2). This leads to increased losses in a phenomenon termed Latent, Virtual, or *Rolling Power*, described first by McMillan [19] and further studied by several authors, e.g. [21], [22]. In [3], we propose a *Latent Power Ratio* (*LPR*) to characterize how Rolling Power and thus efficiency is conditioned by gearbox topology. *LPR* is the ratio between the sum of the absolute values of the rolling powers in all meshings, and the power input to the gearbox. Using the equations developed in [23] to calculate the Rolling Powers (P') in meshings S-Ps, P-Ra, P-Rb, the *LPR* of a generalized Wolfrom-based topology (*PoC#1 to #5,* Fig.3) becomes:

$$LPR = \sum \left|\frac{P_{roll}}{P_{In}}\right| = \left(1 - 2\frac{1}{i_0}\right) + \eta_{Tot} \cdot (2i_W - 1);$$

$$\text{with } i_{Tot} = \frac{\omega_S}{\omega_{Rb}} = i_0 \cdot i_W;\ i_0 = \frac{\omega_S}{\omega_C};\ i_W = \frac{\omega_C}{\omega_{Rb}};$$

where the total gearbox reduction ratio i_{Tot} is decomposed in two terms i_0, i_W and we assume, without loss of generalization, that $i_W > 0$. Using Böge's Geometry Coefficients S_1, S_2, S_3 [24] to relate i_0, i_W to gearbox topology through a gearwheels' number of teeth (Z) leads to:

$$S_1 = \frac{Z_{Ps}}{Z_S}; S_2 = \frac{Z_{Ra}}{Z_{Pa}}; S_3 = \frac{Z_{Rb}}{Z_{Pb}}; i_0 = 1 + S_1 S_2; i_W = \frac{S_3}{S_3 - S_2};$$

In [23] we also demonstrated that higher i_0 reduces the Rolling Power (and thus *LPR*), attenuating the rapid efficiency deterioration with total gear ratio in Wolfrom-based gearboxes, for which efficiency is given by:

$$\eta_{Tot} = \frac{1 + \frac{\mathrm{f}_{L,P-Ra}}{i_0} - \mathrm{f}_{L,S-P}\left(1 - \frac{1}{i_0}\right)}{1 + \mathrm{f}_{L,P-Ra} i_W + \mathrm{f}_{L,P-Rb}(i_W - 1)};$$

where, for a given meshing between pinion *p* and gear *g*, $\mathrm{f}_{L,p-g}$ is the meshing Loss Factor, related to the basic *p-g* meshing efficiency η_{p-g} [25] through:

$$\mathrm{f}_{L,p-g} = 1 - \eta_{p-g};$$

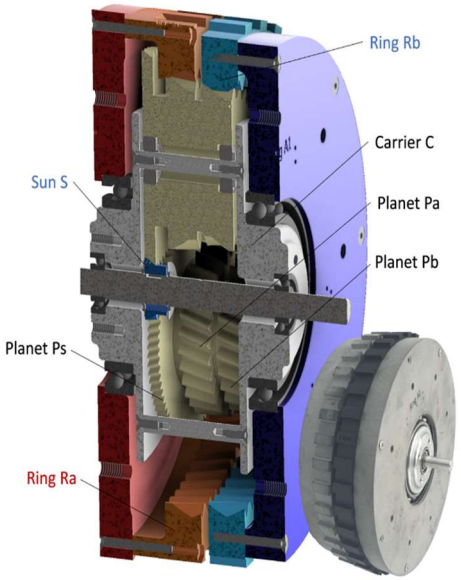

Figure 2. PoC#4 (Φ250 x 102 mm, 4.57kg) gearbox with the Optimized (OptM) topology configuration shown on Fig.3.

In a conventional Wolfrom (*PoC#1, Fig.3*), $Z_{Ps} = Z_{Pa}$ and the ratio i_0 is directly related to S_2 through:

$$S_1 = \frac{1}{(S_2 - 1)} \Rightarrow i_0 = 1 + \frac{S_2}{S_2 - 1}; (1)$$

The maximum i_0 is thus limited by a maximum S_2, itself limited by gearbox's diameter, a minimum functional number of teeth, and tooth size (module) that can withstand the high stresses in the P-Ra meshing. *R2poweR* breaks this direct link between i_0 and S_2 by means of splitting the first stage into two,

such that (i) higher i_0-ratios can be achieved, reducing LPR, and (ii) the tooth macrogeometry of the S-P meshing can be separately optimized. The immediate benefit of this strategy is the cancelation of the poor efficiency of Wolfrom-based gearboxes, removing a main obstacle hindering their large potential to build more compact, lightweight actuators [17].

An additional advantage of splitting the first Wolfrom stage are more balanced Hertzian and bending loads between the gear engagements, ultimately leading to a more compact gearbox [23]. This advantage is not yet explored in this proof-of-concept: the five gearbox configurations described in the next section have been designed to allow a direct comparison of the different *R2poweR* acting principles. Number of teeth (*NOT*) and tooth size (thus gearbox dimensions) are consequently very similar for all *PoC*s. This strategy unfortunately prevented us to exploit the full weight optimization potential of *R2poweR* at this stage.

B. B. The PoC Gearboxes

This *R2poweR* PoC validation compares the efficiency of five different gearbox configurations. Additionally, virtual reference gearboxes are defined, with identical gear ratios and customary basic meshing efficiencies (98% for plastic and 99% for steel [19]) and incorporated to the comparison, to evaluate *R2poweR*'s ability to minimize losses.

Four prototypes are manufactured in larger scale (5:2) with 3D printed (multi-jet fusion) polyamide-12 gearwheels. Previous results [26] showed this to be a simpler yet representative approach to compare load-dependent losses in planetary gearboxes. The *PoC#5* prototype is manufactured in 1:1 scale with conventional gear steel material, to assess the absolute gearbox's efficiency potential and the influences of material and manufacturing processes. All gearwheels are generously lubricated with SUPER-LUBE (steel) and GEAR-FLON (plastic) high-performance grease, with PTFE. Their mechanical interface elements with the bench are common.

Fig.3 shows the schematic configuration of all *PoC* gearboxes, while Table I provides their main parameters. Tooth geometry is optimized for maximum efficiency using the KISSSOFT © software, using low contact ratios and balanced approach and recess arcs, similar to [12]. KISSSOFT © also uses Ohlendorf's model [20] to estimate load-dependent losses. The design pressure angle is 20 degrees for all teeth.

- PoC#1 – *Wolfrom*

The first *PoC* configuration (PoC#1, Fig.3) corresponds to a conventional Wolfrom planetary with a 125:1 gear ratio and efficiency-optimized tooth macrogeometry.

- PoC#2 – *Ferguson* Planetary

This is an interesting variant of the Wolfrom configuration. The compound planets are replaced with a planet with the teeth of the first gearwheel extended along its complete length. The profile shift of Rb is corrected to enable good engagement with the planet and with different *NOT*, negatively conditioning the efficiency-optimization of the tooth geometry. Yet, this design improves manufacturability and cost substantially [27].

- PoC#3 – *Split*

The *Split* configuration implements a first *R2poweR* topology modification. Simultaneous meshing of the planet gearwheel Pa with sun S and ring Ra gearwheels is prevented by means of splitting Pa into two separate gearwheels Ps, Pa. The planet set has now three distinct stages (Ps, Pa, Pb), each meshing with a single gearwheel. Thanks to the relatively small torques in the S-Ps stage, tooth size (module) can be reduced and macrogeometry optimized separately. This improves basic meshing efficiency (99,4% vs. 98.7% in *PoC#1,* calculated with KISSSOFT) in this stage. Note also that the small torques enable very thin gearwheels S, Ps, minimizing the increase of planet length, mass, and inertia.

- PoC#4 – Optimized (*OptM*)

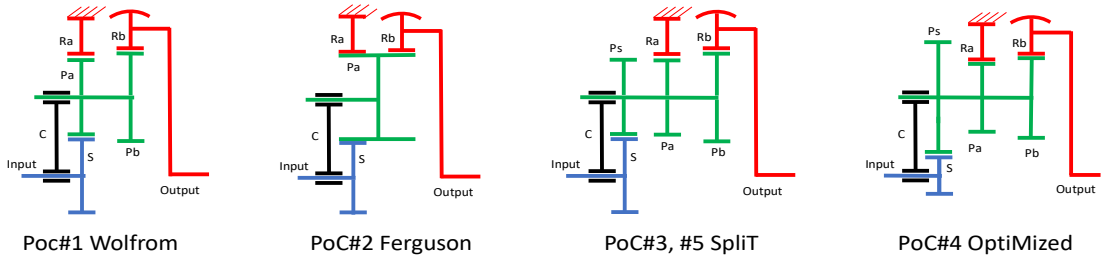

Figure 3. Configuration of the five PoC gearboxes. "S" = Sun gearwheel, "P" = Planet gearwheel, "R" = Ring gearwheel, "C" = carrier element, "a" = first gearbox stage, "b" = final gearbox stage, "s" = pre-stage.

TABLE II. MAIN POC GEARBOX CHARACTERISTICS

PoC Gearbox	Gear Ratio	Scale	Torque	Weight	Gearwheels		Module (mm.) of stage			Number of Teeth					
			Peak (Nm)	*(kg)*	*Material*	*Manufacture*	*"s"*	*"a"*	*"b"*	*S*	*Ps*	*Pa*	*Pb*	*Ra*	*Rb*
PoC#1 - Wolfrom	125:1	5:2	80	4.36	PA12	MultiJet-Fusion	-	2.50	2.35	18	-	27	27	72	75
PoC#2 - Ferguson				4.38			-		2.50		-				
PoC#3 – Split				4.49			1.24		2.35	36	54				
PoC#4 - OptM	275:1			4.57			1.20	2.30	2.40	20	75	30	27	80	
PoC#5 – Split-Steel	125:1	1:1	120	1.56	42CrMo4V	CNC & EDM	0.5	1.00	0.94	36	54	27	27	72	

Note that the numbers of teeth (and modules when possible) have been chosen to be close to each other, to optimize PoC comparability.

In a Wolfrom gearbox, the geometry ratio S_1 is conditioned by a maximum S_2 through equation (1). After splitting, the smaller teeth can be used to reduce the size of the Sun (S) gearwheel and increase S_1. In *PoC#3* this potential was not yet exploited: the smaller module was used instead to increase the Sun's (S) *NOT* from 18 to 36. In *PoC#4* we reduce the Sun *NOT* to 20 to increase S_1 and thus i_0, increasing the diameter of the first stage (204 vs. 179mm) to reach $S_1 = \frac{75}{20} = 3{,}75$ for *PoC#4*, instead of $\frac{54}{36} = 1{,}5$ for *PoC#3*.

Further, instead of reducing i_W to maintain total gear ratio i_{Tot}, *PoC#4* maintains identical geometry ratios S_2, S_3 as *PoC#3*. In this way, the meshings between planet set and rings Ra and Rb are very similar for both prototypes, allowing a more direct comparison. Consequently, i_0 increases to 11 and i_{Tot} to 275:1, to explore *R2poweR*'s with higher reductions.

- PoC#5 – *Steel-Split*

PoC#5 corresponds to the same configuration of *PoC#3* and was included to validate *R2poweR* with conventional gear materials (42CrMo4V) and manufacturing methods. CNC machining (planets) and EDM wire-cutting (ring gearwheels) increased cost, but accuracy and surface finish are not anymore directly conditioned by size, making possible a 1:1 scale.

C. Backdrivability

A further benefit of improved efficiency is improved backdrivability, fundamental in human-robot interaction [3]. Backdrivability corresponds to the actuator's mechanical impedance when driven from the load side, which, for rigid enough actuators, is governed by the combined effect of friction and inertia. Matsuki demonstrated [12] that at moderate accelerations (actuator's inertia is less influential) a substantial efficiency improvement allows easily backdriving a Wolfrom gearbox. At higher accelerations, the actuator's inertia (reflected to the load side) must also be considered.

Fig.4 shows a simple inertia model of a rigid actuator with an electrical motor and a Wolfrom-based gearbox. Grouping the different elements according to their rotating speeds, the mechanical impedance in forward-driving (*Fwd*) and backdriving (*Bck*) can be calculated as a function of the *Fwd*- and *Bck*- efficiencies and of the total system inertias, reflected respectively to motor (*Fwd*-) and to load (*Bck*-):

$$\frac{\tau_{Fwd}}{\dot{\omega}_{Mot}} = \frac{J_{Fwd}}{\eta_{Fwd}};\ J_{Fwd} = J_{M+S} + N\frac{J_P}{\eta_P i_P^2} + \frac{J_C}{\eta_C i_0^2} + \frac{J_{R+L}}{\eta_{Fwd} i_{Tot}^2};$$

$$\frac{\tau_{Bck}}{\dot{\omega}_L} = \frac{J_{Bck}}{\eta'_{Bck}};\ J_{Bck} = J_{R+L} + \eta'_C i_W^2 J_C + N\eta'_P \frac{i_{Tot}^2}{i_P^2} J_P + \eta'_{Bck} i_{Tot}^2 J_{M+S};$$

where $i_P = \frac{\omega_M}{\omega_P - \omega_C}$, while $\eta_{Fwd}, \eta_C, \eta_P, \eta'_{Bck}, \eta'_C, \eta'_P$ must be incorporated to account for torque losses between the torque input to the system and the torque available respectively at carrier (*C*), planet (*P*), and system output, both in *Fwd* (η) and *Bck* (η') directions, N= number of planets, and J_k is the inertia of the *k*- element in:

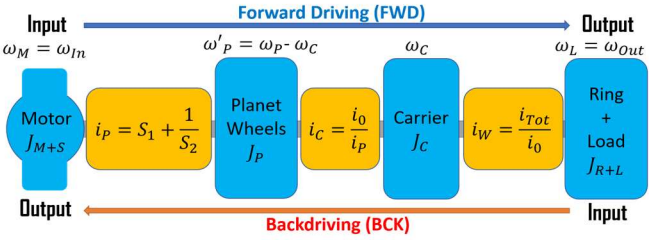

Figure 4. General Inertia Model of a system with an actuator including a Wolfrom-based gearbox and an electrical motor

- k = M+S: elements rotating at ω_{In}, that is, the motor's rotor and the gearbox's input shaft, including the sun (S) gearwheel and inner rings of its bearings
- k = P: elements rotating at $\omega_P - \omega_C$, that is, planet gearwheels and their bearings' outer rings
- k = C: elements rotating at ω_C, that is, the carrier assembly including its pins and bearings, but also the planet gearwheels (due to their composed rotation around their own axis and around that of the gearbox).
- k = R+L: elements rotating at ω_{Out}, that is, the ring B (Rb) gearwheel, and the external load (L)

III. Method

Previous experiences [26] indicated that measuring gearbox efficiency is a particularly challenging endeavor. A fast enough sampling rate is required to allow the control system maintaining constant and accurate speeds. At the same time, torque sensing accuracy is strongly affected by the sensor's vibration, attached to a rotating shaft and subject to the effects of transmission errors and speed/torque control adjustments. We selected a hoist-like rig configuration in which the gearbox is connected to a motor and lifts a calibrated weight, instead of using a conventional servo-brake load. With this simpler and economic set-up, similar accuracy can be achieved. Further, gearbox loading consists of a pure output torque and an additional tilting torque that makes it more representative of real loading as part of a robotic device. The set-up and its underlying configuration are shown in Fig.5.

Accurate knowledge of the calibrated weight and the dimensions of the drum connected to the gearbox allow for a reasonable estimation of the torque payload that is not directly affected by sensing accuracy. Although the accuracy of this method is affected by the model truthfulness and thus the bearing reactions, those can be neglected particularly when comparing gearboxes to each other, in equivalent operating points. Thus, using only one torque sensor to measure the motor torque input to the gearbox, we can calculate the torque-output to torque-input ratio and compare it to the gearbox's kinematic gear ratio, to estimate the gearbox efficiency. Operating the gearbox in this exact configuration without load, the no-load losses can also be established and deducted from the overall losses, to determine load-dependent efficiency.

A repeatability check confirmed the need to warm up the gearbox – operating it for over one minute – to achieve good repeatability. Under these premises, the average repeatability error was 0.89% and the maximum error (at high speed and low torques, where dynamics are more relevant, and the sensor's relative accuracy is lower) found was 1.79%.

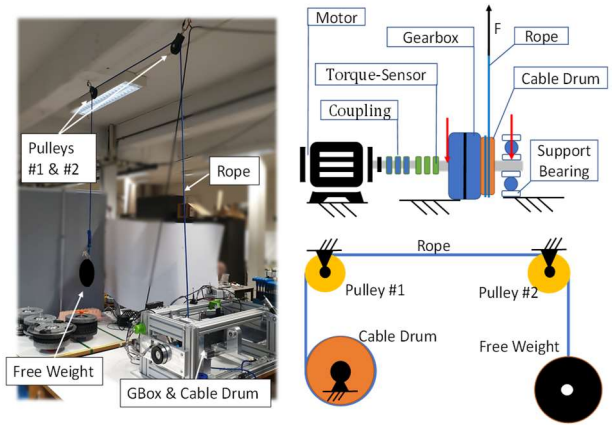

Figure 5. Overall configuration of the Hoist-like test set-up used to measure the efficiency of the PoC gearboxes

A. Test Set-Up

A 600Watt Maxon EC90 flat motor (ref. 597974) incorporating a 2-channel, 2048cpt MILE encoder was controlled using a Maxon EPOS4 70/15 controller with a soft speed-regulation control selection. This controller uses a cascaded control algorithm with a 25kHz PI current controller in the inner loop and a 2.5kHz PI velocity controller in the outer loop. The EC90 motor is connected to the gearbox through a Lorenz DR-2112-M220 torque sensor with a ±2Nm nominal range and an improved accuracy class of 0,05%.

Simulink on a laptop PC controls an EtherCAT, real-time (1kHz) network in a Beckhoff Twin CAT master environment interfacing directly with Simulink [28]. Through the EtherCAT network, the Beckhoff system can control and collect data from the EPOS controller. At the same time, a Beckhoff EL3104 A/D converter collects input torque data from the torque sensor to the EK1100 EtherCAT coupler.

B. Validation Plan

After warming up under load for two minutes, each prototype is tested at five input speeds (250, 500, 1000, 1500, 2000rpm) in four different load conditions (no-load, 5kg/4.9Nm, 15kg/14.3Nm, 25kg/23.6Nm). The test is run twice for each of the 20 operating points per *PoC*.

C. Signal Conditioning

The input torque signal is conditioned using a low-pass, anti-aliasing SINC3 filter with a 50Hz cut-off frequency incorporated into the KL3104 Beckhoff A/D converter. This provides sufficient attenuation (60dB) at the 500Hz Nyquist frequency. Additionally, a FIR filter is used to attenuate all harmonics of the 50Hz A/C network frequency.

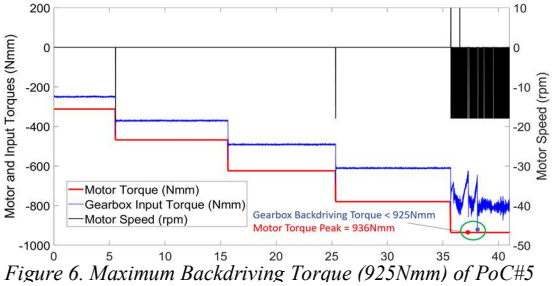

Figure 6. Maximum Backdriving Torque (925Nmm) of PoC#5

Input torque data is collected in each operating point. The initial data is cut-off to allow stabilization and averaged during a complete gearbox rotation. The ratio between calculated torque output and mean input torque is averaged in two test runs and used to estimate gearbox efficiency.

IV. RESULTS

Test results are summarized in Table II and Figs. 6,7, and 8.

TABLE II. EFFICIENCY RESULTS

PoC Gearbox	**Total Efficiency**	**Load-dependent Efficiency**		
	Measured in Experiment	***Reference Gearbox***	***Calculated (Kisssoft)***	***Measured in Experiment***
PoC#1 *Wolfrom*	43%	49.1%	80.0%	75%
PoC#2 *Ferguson*	35%	49.1%	65.4%	67%
PoC#3 *Split*	40%	49.1%	80.6%	77%
PoC#4 *OptM*	28%	30.6%	80.9%	85%
PoC#5 *Split-Steel*	69%	66.2%	87.0%	74%

Measured efficiencies correspond to the averaged results of the tests for both *Load-dependent* and *Total efficiencies*. *Reference* values are calculated using Ohlendorf's model and a customary basic meshing efficiency (99% for steel and 98% for plastic gearwheels) that corresponds to conventional tooth geometries, not optimized for efficiency and not including any topology optimization ($i_0 = 5$). *Calculated* values are determined for each configuration using also Ohlendorf's model in Kisssoft, with tooth-geometry optimized this time for efficiency (low contact-ratio and balanced approach and recess arcs), corresponding to the tooth geometry ultimately incorporated to the PoC prototypes and measured.

Table II compares the efficiency of all *PoC* prototypes and reference gearboxes (same gear ratio, non-optimized topology with $i_0 = 5$, and customary macrogeometry with 99% basic meshing efficiency (98% for plastic) [18]:

- (*Measured)* load-dependent efficiency improved strongly for all prototypes, compared to their *reference* gearboxes.
- *OptM* (*PoC#4*) results demonstrate that splitting the first stage of a Wolfrom configuration to optimize topology and macrogeometry enables very high ratios (275:1) with high load-dependent efficiency (85%).
- The last two columns show a good correlation between Ohlendorf's estimations and empirical results. Yet, this model does not explain all relative changes (*Split* to *OptM, Wolfrom* to *Ferguson*). Similar limitations had already been previously documented by other researchers [29].
- *Measured* load-dependent efficiency is substantially lower than *calculated* for *PoC#5* (74% vs. 87%). No-load losses were reduced (Fig.8) leading to 69% total efficiency.
- *PoC#2* shows the lowest load-dependent efficiency and requires the largest input torques in Fig.8, yet the *measured*

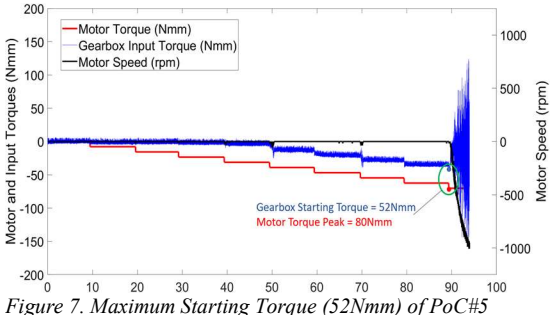

Figure 7. Maximum Starting Torque (52Nmm) of PoC#5

detrimental impact of the simpler *Ferguson* configuration is significantly smaller than *calculated* using Ohlendorf's model with KISSSOFT.

The maximum backdriving and starting torques of PoC#5 are respectively 925Nmm and 52Nmm, Figs. 6 and 7.

V. Discussion

A limitation of this study is the model's inability to accurately explain all the efficiency differences, and the effect of pulley losses in the results. Although this does not fundamentally alter the representativity of the efficiency comparison between *PoC* configurations, a rapid calculation using Palmgrens' model [30] to evaluate load-dependent and viscous friction torques indicates that the total efficiencies of the *PoC* gearboxes could be between 2% and 4% higher.

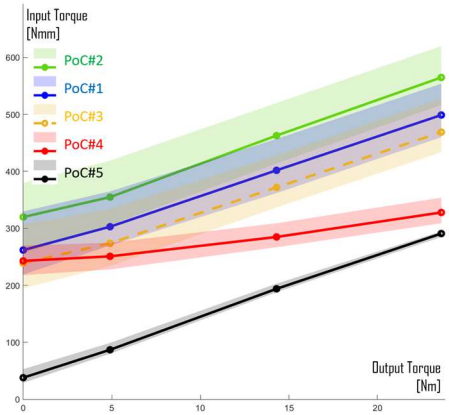

Figure 8. For a given payload (output torque), the lines indicate the required Input Torque (at 1000 rpm) for each prototype. The colored bands show the input torque spread as input speed varies from 250rpm (lower limit) to 2000rpm (higher limit). PoC#5 shows the lowest input torque (highest total efficiency) and thinnest band (lowest speed dependency). The flatter trend of PoC#4 indicates lower load-dependent efficiency, due to the higher ratio. PoC#2 shows highest input torque (highest losses) and the broadest band (high speed dependency). PoC#3 and PoC#5 show the effect of different scale, materials, and manufacturing methods on a shared configuration: the curves correlate well to each other in terms of slope (load-dependent efficiency) while highlighting the improvement in no-load losses and on the speed-dependency of efficiency f PoC#5.

We hypothesize the lower-than-expected load-dependent efficiency of *PoC#5* to result from uneven load distribution between its over-constrained planets, complicated by a higher material stiffness of steel. This correlates well with VDI-2736 recommendation to disregard, due to higher elasticity of thermoplastics, the effect of manufacturing inaccuracies and pitch deviations ($K_{F\alpha}$, $K_{F\beta}$) on uneven load distribution [34].

Another fundamental finding is the relatively low (925Nmm) backdriving torque of *PoC#5, Fig.6*, confirming that Wolfrom gearboxes with macrogeometry upgraded for efficiency have substantially lower backdriving torques than HD and CD gearboxes (Fig.9). Combined with the backdriving-inertia advantage resulting from using a lightweight motor, this result shows that high reduction ratios are not incompatible with good backdrivability, as it is often assumed in robotics.

Table III compares the performance of *PoC#5 Steel-Split* with state-of-the-art, commercially available *HD CSG-20-120* and *SPINEA's TS80 CD* gearboxes with close operational characteristics. Despite the low TRL maturity (TRL4) and rapid-prototype manufacture, *PoC#5* achieves benchmark efficiency and shows better efficiency at lower loads, a valuable asset in robotics, where operation at partial loads is frequent [31]. Mass and dimensions are also very promising, considering the focus on testbench compatibility and prototype comparability, and not yet on minimizing weight or size.

TABLE III. Performance Comparison of PoC#5 with commercial Harmonic Drive [32] & Cycloid Drive [33] Gearboxes

Model	Gear Ratio	Torque (Nm)	Φ (mm)	Width (mm)	Weight (gr)	Efficiency @ (Nm)		
						23.6	13.5	4.9
HD CSG 20-120	120:1	113	93	46	980	65%	55%	33%
CD TS80	85:1	156	80	47	1640	64%	51%	27%
PoC#5	125:1	120	98	68	1560	69%	62%	48%

VI. Conclusion

These tests provide a first proof-of-concept demonstration of *R2poweR*'s capacity to substantially improve efficiency in Wolfrom-based gearboxes, combining topology optimizations to reduce *Latent Power Ratios* with efficiency-optimized tooth geometries, enabling *R2poweR's* progress to TRL4 maturity.

Future research will focus on validating this promising potential in higher TRLs, combining the *OptM* topology (*PoC#4*) with conventional gear materials and advanced manufacturing processes in an advanced prototype. Optimized for minimum weight and with a higher reduction (around 275:1), this TRL6 prototype could be combined with a lighter EC60 motor to achieve maximum torque density. Assuming basic meshing efficiencies, close to those estimated by KISSSOFT, benchmark efficiency, size, weight, and backdrivability could be reached. Figure 9 summarizes these TRL6 performance objectives and compares them to those of the *PoC#5* and to commercial Harmonic and Cycloid Drives.

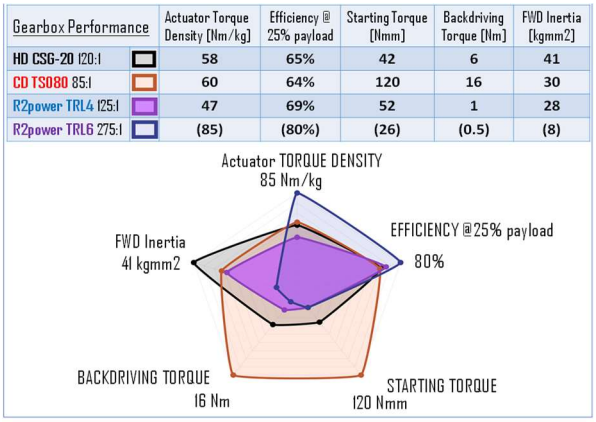

Figure 9. Performance Objective (in brackets) for a future TRL6 prototype, compared to measured values at TRL4 (PoC#5) and to lightweight Harmonic Drive [32] and Cycloid Drive [33] commercial gearboxes.

Future research will also focus on trying to upgrade Ohlendorf's efficiency model to improve its accuracy predictions for high-ratio planetary gearboxes, characterized by large *Rolling Power* (high *LPR*). We will attempt this using a back-to-back, mechanically-closed-loop test bench [35] for high-ratio planetary gearboxes, capable of more accurate efficiency measurements than our hoist-based testbench.

REFERENCES

[1] Siciliano, B., Sciavicco, L., Villani, L., & Oriolo, G. *Robotics: modelling, planning, and control*. Springer Science and Business Media, 2010.

[2] International Federation of Robotics, Executive Summary World Robotics 2020: Service Robots, 2020.

[3] Lopez Garcia, P., Crispel, S., Saerens, E., Verstraten, T., & Lefeber, D. "Compact gearboxes for modern robotics: A review." *Frontiers in Robotics and AI, 7, 103*, August 2020.

[4] Ishida, T., & Takanishi, A. "A robot actuator development with high backdrivability." In 2006 *IEEE Conference on Robotics, Automation and Mechatronics (pp. 1-6)*, June 2006.

[5] Wang, J., Li, X., Huang, T. H., Yu, S., Li, Y., Chen, T., & Su, H. "Comfort-centered design of a lightweight and backdrivable knee exoskeleton." *IEEE Robotics and Automation Letters*, 3(4), 4265-4272, 2018.

[6] Sensinger, J. W., "Efficiency of high-sensitivity gear trains, such as cycloid drives." *Journal of Mechanical Design*, 135(7), 071006, 2013.

[7] Kenneally, G., De, A., & Koditschek, D. E., "Design principles for a family of direct-drive legged robots." *IEEE Robotics and Automation Letters*, 1(2), 900-907, 2016.

[8] Zhu, H., Nesler, C., Divekar, N., Peddinti, V., & Gregg, R., "Design Principles for Compact, Backdrivable Actuation in Partial-Assist Powered Knee Orthoses.", *IEEE/ASME Transactions on Mechatronics*, 2021.

[9] Chignoli, M., Kim, D., Stanger-Jones, E., & Kim, S., "The MIT Humanoid Robot: Design, Motion Planning, and Control For Acrobatic Behaviors.", *arXiv preprint* arXiv:2104.09025, 2021

[10] Elery, T., Rezazadeh, S., Nesler, C., & Gregg, R. D. "Design and validation of a powered knee–ankle prosthesis with high-torque, low-impedance actuators." *IEEE Transactions on Robotics, 36(6), 1649-1668*, 2020.

[11] Wensing, P. M., Wang, A., Seok, S., Otten, D., Lang, J., & Kim, S. (2017). "Proprioceptive actuator design in the MIT cheetah: Impact mitigation and high-bandwidth physical interaction for dynamic legged robots." *IEEE Transactions on Robotics, 33(3), 509-522*, 2017.

[12] Matsuki, H., Nagano, K., & Fujimoto, Y., "Bilateral drive gear—a highly backdrivable reduction gearbox for robotic actuators." *IEEE/ASME Transactions on Mechatronics*, 24(6), 2661-2673, 2019.

[13] Höhn, B. R., Zhang, Y., Geitner, M., & Otto, M., "A Wolfrom transmission without carrier.", *MATEC Web of Conferences* , 317, p. 01001), 2020.

[14] Wolfrom, U.: *Der Wirkungsgrad von Planetenrädergetrieben*. Werkstattstechnik, Vol. VI, 1912.

[15] Saerens, E., Crispel, S., Garcia, P. L., Verstraten, T., Ducastel, V., Vanderborght, B., & Lefeber, D., "Scaling laws for robotic transmissions." *Mechanism and Machine Theory*, 140, 601-621, 2019.

[16] Verstraten, T., Furnémont, R., Mathijssen, G., Vanderborght, B., & Lefeber, D., "Energy consumption of geared DC motors in dynamic applications: Comparing modelling approaches.", *IEEE Robotics and Automation Letters*, 1(1), 524-530, 2016.

[17] Kapelevich, A., & AKGears, L. L. C. "High gear ratio epicyclic drives analysis." *Gear Technology*, 3 (10), June 2014.

[18] Niemann, G., & Winter, H., *Maschinenelement Band 2: Getriebe allgemein, Zahnradgetriebe – Grundlagen, Stirnradgetriebe*. Springer -Verlag, Berlin-Heidelberg, 2003.

[19] Macmillan, R. H., "Power flow and loss in differential mechanisms." *Journal of Mechanical Engineering Science*, 3(1), 37-41, 1961.

[20] Ohlendorf, H., „Verlustleistung und Erwärmung von Stirnrädern." Doctoral Dissertation, Technische Universität München, 1958.

[21] Chen, D. Z., & Tsai, L. W. "Kinematic and dynamic synthesis of geared robotic mechanisms", *ASME Journal of Mechanical Design*, 115(2): 241–246, June 1993.

[22] Esmail, E. L., Pennestrì, E., & Cirelli, M., "Power-Flow and Mechanical Efficiency Computation in Two-Degrees-of-Freedom Planetary Gear Units: New Compact Formulas", *Applied Sciences*, 11(13), 5991, 2021.

[23] Crispel, S., Lopez Garcia, P., Saerens, E., Varadharajan, A., Verstraten, T., Vanderborght, B., & Lefeber, D. "A Novel Wolfrom-based Gearbox for Robotic Actuators." *IEEE/ASME Transactions on Mechatronics*, 2021.

[24] Böge, A., & Schlemmer, W.: *Die Mechanik der Planetengetriebe,* Vieweg, 1980.

[25] Velex, P., & Ville, F., "An analytical approach to tooth friction losses in spur and helical gears—influence of profile modifications.", *Journal of Mechanical Design*, 131(10), 2009.

[26] Lopez Garcia, P., Crispel, S., Verstraten, T., Saerens, E., Vanderborght, B., & Lefeber, D., "Customizing planetary gear trains for human limb assistance and replication", *MATEC Web of Conferences* , Vol. 287, p. 01014, 2019.

[27] Arnaudov, K., Karaivanov, D.P., *Planetary Gear Trains*, CRC Press, 2019.

[28] Langlois, K., van der Hoeven, T., Cianca, D. R., Verstraten, T., Bacek, T., Convens, B., Vanderborght, B., "Ethercat tutorial: An introduction for real-time hardware communication on windows." *IEEE Robotics & Automation Magazine*, 25(1), 22-122, 2018.

[29] Wimmer, J. A. „Lastverluste von Stirnradverzahnungen: Konstruktive Einflüsse, Wirkungsgradmaximierung, Tribologie," Doctoral Dissertation, Technische Universität München, 2006.

[30] Palmgren, A., *Ball and roller bearing engineering*. Philadelphia: SKF Industries Inc., 1959.

[31] Verstraten, T., Mathijssen, G., Furnemont, R., Vanderborght, B., & Lefeber, D. (2015). "Modelling and design of geared DC motors for energy efficiency: Comparison between theory and experiments." Mechatronics, 30, 198-213

[32] Reducer Catalog of Gear Units CSG/CSF, *Harmonic Drive LLC*, September 2019.

[33] TwinSpin and DriveSpin Reducer Catalogue, *Spinea s.r.o*, 2019.

[34] ISO 6336:2019 Parts 1-6, Calculation of load capacity of spur and helical gears, 2019.

[35] Mihailidis, A., & Nerantzis, I., "A new system for testing gears under variable torque and speed.", *Recent Patents on Mechanical Engineering*, 2(3), 179-192, 2009.